PATTERNING OF GaN IN HIGH-DENSITY Cl_2- AND BCl_3-BASED PLASMAS

[a]R. J. Shul, [a]R. D. Briggs, [a]J. Han, [b]S. J. Pearton, [b]J. W. Lee, [b]C. B. Vartuli, [c]K. P. Killeen, and [c]M. J. Ludowise

[a]Sandia National Laboratories, Albuquerque, NM 87185-0603, rjshul@sandia.gov
[b]University of Florida, Department of Materials Science and Engineering, Gainesville, FL 32611
[c]Hewlett-Packard Laboratories, Palo Alto, CA 94304

ABSTRACT

Fabrication of group-III nitride electronic and photonic devices relies heavily on the ability to pattern features with anisotropic profiles, smooth surface morphologies, etch rates often exceeding 1 μm/min, and a low degree of plasma-induced damage. Patterning these materials has been especially difficult due to their high bond energies and their relatively inert chemical nature as compared to other compound semiconductors. However, high-density plasma etching has been an effective patterning technique due to ion fluxes which are 2 to 4 orders of magnitude higher than conventional RIE systems. GaN etch rates as high as ~1.3 μm/min have been reported in ECR generated ICl plasmas at -150 V dc-bias. In this study, we report high-density GaN etch results for ECR- and ICP-generated plasmas as a function of Cl_2- and BCl_3-based plasma chemistries.

INTRODUCTION

Interest in GaN and related group-III nitride materials continues to grow as demonstrations of blue, green, and ultraviolet (UV) light emitting diodes (LEDs), blue lasers, and high temperature electronic devices are reported.[1-16] Fabrication of many of theses devices may be attributed to improvements in material growth capabilities. However, enhanced device performance can only be realized with improved process capabilities, including plasma etch. Although many advances in plasma etch technology have transpired, the rapid development of high-performance state-of-the-art devices, sub-0.5 μm features, and complex material structures, including the group-III nitrides, has increased the requirements for etch processes. Plasma etch processes often demand highly anisotropic profiles, high etch rates, smooth morphologies, and low-damage. Etching the group-III nitrides is further complicated by their inert chemical nature and their strong bond energies as compared to other compound semiconductors. GaN has a bond energy of 8.92 eV/atom, InN 7.72 eV/atom, and AlN 11.52 eV/atom as compared to GaAs which has a bond energy of 6.52 eV/atom. Due to these high bond energies and inert chemical behavior, the group-III nitrides resist etching in standard, room temperature wet chemical etchants. Therefore, essentially all device patterning has been accomplished using plasma etching technology. For example, commercially available LEDs from Nichia are fabricated using a Cl_2-based RIE to expose the n-layer of the heterostructure.[1, 2, 5] The first GaN-based laser diode was also fabricated using RIE to form the laser facets.[7] Laser facet fabrication is especially dependent upon plasma etch pattern transfer since the majority of epitaxially grown group-III nitrides are on sapphire substrates which inhibits cleaving the sample with reasonable yield.

Perhaps the most significant advancement in plasma etching the group-III nitrides has been the utilization of high-density plasmas. High-density plasma etch systems typically yield higher etch rates with less damage than more conventional reactive ion etch (RIE) systems due to plasma densities which are 2 to 4 orders of magnitude greater and the ability to effectively decouple ion energies and plasma density. Etch profiles also tend to be more anisotropic due to lower process pressures which results in less collisional scattering of the plasma species. Plasma etching of GaN has been reported using several techniques including RIE, electron cyclotron resonance (ECR), inductively coupled plasma (ICP), magnetron reactive ion etch (MIE) systems, and chemically assisted ion beam etching (CAIBE). In this paper, we compare ECR and ICP etch results for GaN in Cl_2- and BCl_3-based plasmas. Etch rates, profiles, near-surface stoichiometry, and surface and sidewall morphology will be discussed.

EXPERIMENT

The GaN films etched in this study were grown by one of three techniques; metal organic-molecular beam epitaxy (MO-MBE), radio-frequency-MBE (rf-MBE), or metal organic chemical vapor deposition (MOCVD). The ECR plasma reactor used in this study was a load-locked Plasma-Therm SLR 770 etch system with a low profile Astex 4400 ECR source in which the upper magnet was operated at 165 A. Due to the magnetic confinement of electrons within the microwave source (2.45 GHz), high-density plasmas are formed at low pressures with low plasma potentials and ion energies. Highly anisotropic etching can be achieved by superimposing an rf-bias (13.56 MHz) on the sample and employing low pressure conditions (≤5 mTorr) which minimizes ion scattering and lateral etching. With rf-biasing, energetic ions are accelerated from the plasma to the sample with potential for kinetic damage to the surface. Etch gases were introduced through an annular ring into the chamber just below the quartz window. To minimize field divergence and to optimize plasma uniformity and ion density across the chamber, an external secondary collimating magnet was located on the same plane as the sample and was run at 25 A. Plasma uniformity was further enhanced by a series of external permanent rare-earth magnets located between the microwave cavity and the sample.

ICP offers an alternative high-density plasma technique where plasmas are formed in a dielectric vessel encircled by an inductive coil into which rf-power is applied.[17, 18] The electric field produced by the coils in the horizontal plane induces a strong magnetic field in the vertical plane trapping electrons in the center of the chamber and generating a high-density plasma. At low pressures (≤ 20 mTorr), the plasma diffuses from the generation region and drifts to the substrate at relatively low ion energy. Thus, ICP etching is also expected to produce low damage with high etch rates. The ICP reactor used in this study was a load-locked Plasma-Therm SLR 770 with a cylindrical coil configuration and alumina vessel encircled by a three-turn inductive coil into which 2 MHz rf-power was applied As with ECR etching, anisotropic profiles were obtained by superimposing a rf-bias (13.56 MHz) on the sample to independently control ion energy. Etch gases were introduced through an annular region at the top of the chamber. The general belief is that ICP sources are easier to scale-up than ECR sources and are more economical in terms of cost and power requirements. ICP does not require the electromagnets or waveguiding technology necessary in ECR. Additionally, automatic tuning technology is much more advanced for rf-plasmas than for microwave discharges.

All samples were mounted using vacuum grease on an anodized Al carrier that was clamped to the cathode and cooled with He gas. Samples were patterned using AZ 4330 photoresist. Etch rates were calculated from the depth of etched features measured with a Dektak stylus profilometer after the photoresist was removed with an acetone spray. Each sample was ~1 cm^2 and depth measurements were taken at a minimum of three positions. Standard deviation of the etch depth across the sample was nominally less than ± 10% with run-to-run variation less than ± 10%. The gas phase chemistry for several plasmas was studied using a quadrupole mass spectrometer (QMS) or an optical emission spectrometer (OES). Surface morphology, anisotropy, and sidewall undercutting were evaluated with a scanning electron microscope (SEM). The root-mean-square (rms) surface roughness was quantified using a Digital Instruments Dimension 3000 atomic force microscope (AFM) system operating in tapping mode with Si tips. Auger electron spectroscopy (AES) was used to investigate the near-surface stoichiometry of GaN before and after exposure to several plasmas.

RESULTS AND DISCUSSIONS

Due to their inert chemical nature and high bond strengths, the group-III nitrides resist etching in common compound semiconductor wet chemical etchants at room temperature. Very slow etching of GaN has been reported in hot alkalis or electrolitically in NaOH.[19, 20] InN etch rates of 300-600 Å/min have been reported in aqueous KOH and NaOH at 60°C.[21, 22] For amorphous or polycrystalline AlN, wet chemical etching has been reported in several different solutions including H_3PO_4, HF/H_2O, HNO_3/HF, and dilute NaOH at relatively low rates (≤500 Å/min).[23-29] Mileham *et al.* have recently compiled etch results for binary group-III nitrides in a series of wet chemical

DISCLAIMER

etchants.[30] GaN and InN did not etch in either acid or base solutions below ~80°C. However, single crystal AlN etched in strong KOH- and NaOH-based solutions at room temperature. The etch was strongly dependent upon etchant concentration, temperature, and film quality. Higher etch rates were reported for lower crystalline quality material possibly due to more defects or dangling bonds with which OH^- ions in the etch solution can interact..

Plasma etching of GaN has been reported using several dry etch techniques including RIE, ECR, ICP, MIE, and CAIBE. Using RIE, GaN etch rates as high as 650 Å/min have been reported at dc-biases of -400 V.[31-34] Under similar dc-bias conditions, high-density plasmas typically yield higher etch rates than RIE due to ion densities which are 2 to 4 orders of magnitude greater. Etch profiles also tend to be more anisotropic due to lower process pressures which results in less collisional scattering of the plasma species. GaN etch rates have been reported up to 1.3 µm/min at -150 V dc-bias in an ECR,[35-41] 3500 Å/min at -100 V dc-bias in a MIE,[42] 2100 Å/min at -500 V in a CAIBE,[43] and 6875 Å/min at -280 V dc-bias in an ICP.[44] GaN has also been etched using low energy electron enhanced etching (LE4) at ~2500 Å/min in Cl_2 at 100°C and 0 V dc-bias.[45]

Several different plasma chemistries have been used to etch compound semiconductor materials including halogen- and hydrocarbon-based plasmas. Chlorine-based plasmas have been the dominant etch chemistries used due to the higher volatility of the group-III chlorides as compared to the other halogen-based plasmas. Table I shows boiling points for possible GaN etch products etched in halogen- and hydrocarbon-based plasma chemistries. GaN typically etches at much slower rates than GaAs. The high volatilities of the Ga- and the nitrogen-based etch products shown in Table I implies that the etch rates are not limited by desorption of the etch products. However, due to the strong bond energies of the group-III nitrides, the initial bond breaking of the group-III-N bond, which must precede the etch product formation, may be the rate limiting step.[46] Faster GaN etch rates obtained in high-density plasma etch systems as compared to RIE may be explained by a two step process directly related to the plasma flux and the bond breaking step. Initially the high-density plasmas increase the bond breaking mechanism allowing the etch products to form and then produce efficient sputter desorption of the etch products.

Etch Products	Boiling Point (°C)
$GaCl_3$	201
GaF_3	~1000
$GaBr_3$	279
GaI_3	sub 345
$(CH_3)_3Ga$	55.7
NCl_3	<71
NF_3	-129
NBr_3	na
NI_3	explodes
NH_3	-33
N_2	-196
$(CH_3)_3N$	-33

Table 1. Boiling points for possible etch products of GaN etched in halogen- or CH_4/H_2-based plasmas.

Although fast GaN etch rates have been observed in chlorine-based plasmas, the source of reactive Cl as well as the use of additive gases are important. Very often gas mixtures are used in a plasma to increase etch rate, improve anisotropy, increase selectivity, or produce smoother etch morphologies by adjusting the chemical:physical ratio of the etch mechanism. The addition of Ar,

SF_6, N_2, or H_2 can have a significant effect on the etch characteristics of GaN as can be seen from Table I and are discussed in the following sections.

Small amounts of Ar are often added to halogen-based plasmas to improve the sputter desorption efficiency of etch products from the substrate surface thus increasing etch rate and anisotropy. GaN etch rates are shown in Figure 1 as a function of %Ar in ICP- and ECR-generated Cl_2 plasmas. The plasma etch conditions were 2 mTorr pressure, 30 sccm total flow rate, ~-250 V dc-bias, 25°C substrate temperature, and 500 W ICP source power or 850 W ECR source power. As Ar was added to either ICP or ECR Cl_2 discharges, GaN etch rates decreased due to less available reactive Cl in the plasma. When BCl_3 was substituted for Cl_2, etch rates were relatively constant as function of %Ar and as much as 6 times slower than those obtained in the Cl_2/Ar plasma due to lower concentrations of reactive Cl.

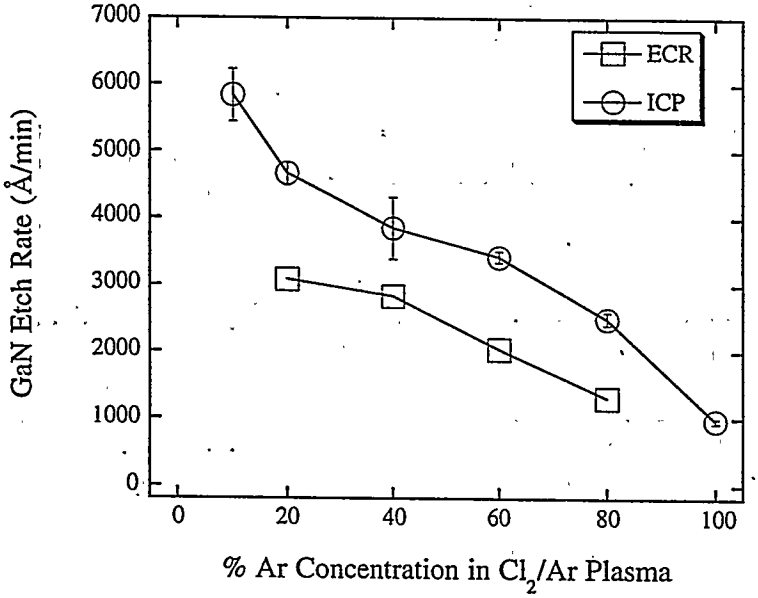

Figure 1. GaN etch rates as a function of %Ar for ECR- and ICP-generated Cl_2/Ar plasmas.

In Figures 2 and 3, GaN etch rates are shown for ECR- and ICP-generated Cl_2/SF_6/Ar and BCl_3/SF_6/Ar plasmas as a function of $\%SF_6$. ECR plasma conditions were; 1 mTorr pressure, 850 W ECR source power, 150 W rf-cathode-power with a corresponding dc-bias of -190 ± 20 V, 25 sccm Cl_2/SF_6 or BCl_3/SF_6, and 5 sccm Ar. ICP plasma conditions were; 2 mTorr pressure, 500 W ICP source power, 95 to 115 W rf-cathode-power with a constant dc-bias of -250 ± 10 V, 25 sccm Cl_2/SF_6 or BCl_3/SF_6, and 5 sccm Ar. (The pressure increased to ~3 mTorr in the ICP reactor at >60% SF_6). In general, as the $\%SF_6$ was increased, the etch rates decreased independent of etch technique. As the $\%SF_6$ was increased from 0 to 20 in the ECR, the Cl concentration, as determined by QMS (indicated by m/e = 35 peak intensity), decreased but remained significant. Faster GaN etching at 20% SF_6 might be expected based on the Cl concentration alone. However, formation of SCl (m/e = 67) was observed at 20% SF_6 which may have been responsible for the reduced GaN etch rate due to consumption of the reactive Cl by S. At 30 and 40% SF_6, the Cl concentration was greatly reduced and slow GaN etch rates resulted. In Figure 3, GaN etch rates increased up to 20% SF_6 in the ICP and 30% SF_6 in the ECR and then decreased sharply in both reactors. In the ECR, the Cl concentration (m/e = 35) increased as the SF_6 increased to 30% and then decreased at 40%. This implied that at low SF_6 concentrations, the SF_6 enhanced the dissociation of BCl_3 resulting in higher concentrations of reactive Cl and faster etch rates. However above ~30% SF_6, the sulfur appeared to consume reactive chlorine as the SCl concentration increased and the etch rate decreased.

GaN etch rates were also obtained for Cl_2/N_2/Ar and BCl_3/N_2/Ar plasmas under the following ECR and ICP conditions; 2 mTorr pressure, 850 W ECR source power or 500 W ICP source

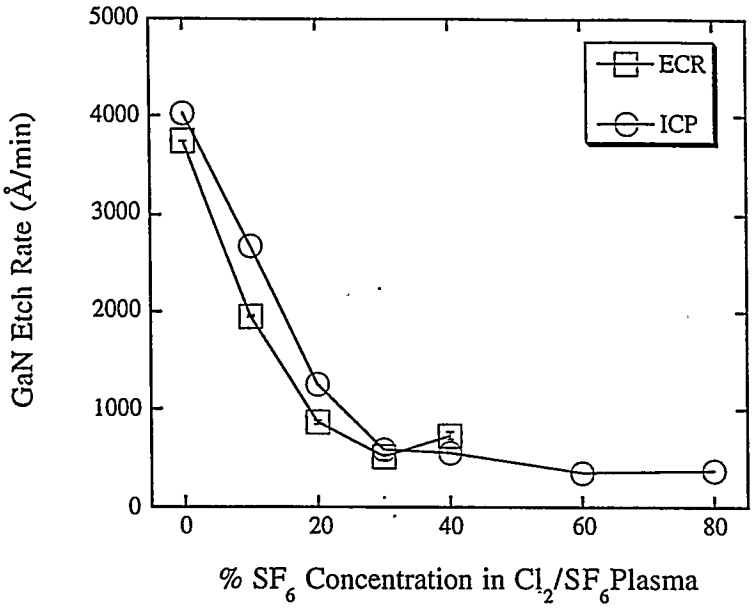

Figure 2. GaN etch rates as a function of %Ar for ECR- and ICP-generated $Cl_2/SF_6/Ar$ plasmas.

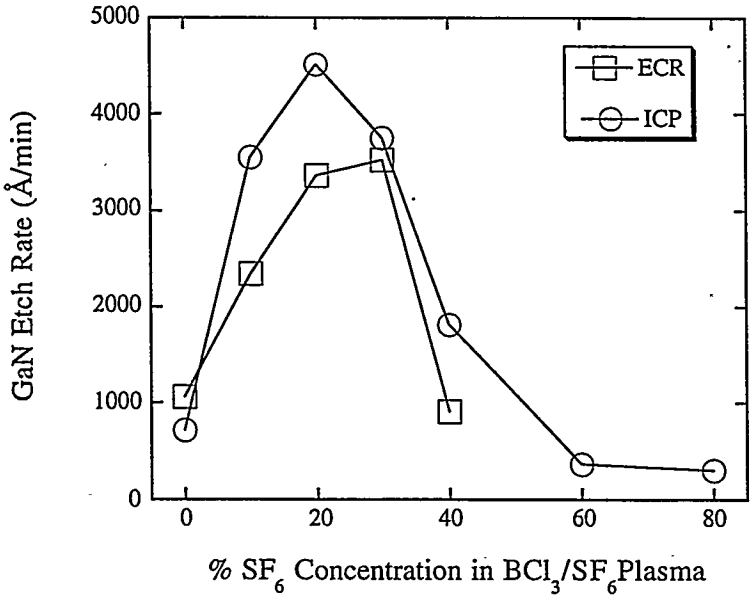

Figure 3. GaN etch rates as a function of %Ar for ECR- and ICP-generated $BCl_3/SF_6/Ar$ plasmas. rates

power, 110 to 170 W rf-cathode-power with a constant dc-bias of -200 ± 10 V, 25 sccm Cl_2/N_2 or BCl_3/N_2, and 5 sccm Ar. Figure 4 shows GaN etch rates as a function of $\%N_2$ concentration in both ECR and ICP Cl_2 plasmas. As the $\%N_2$ increased in the Cl_2 plasma, the GaN etch rates decreased due to less available reactive Cl. However, as shown in Figure 5, GaN etch rates increased significantly as N_2 was added to the ECR- and ICP-generated BCl_3 plasma. Etch rates increased up to 40% N_2 and then decreased at higher N_2 concentrations. This trend was similar to

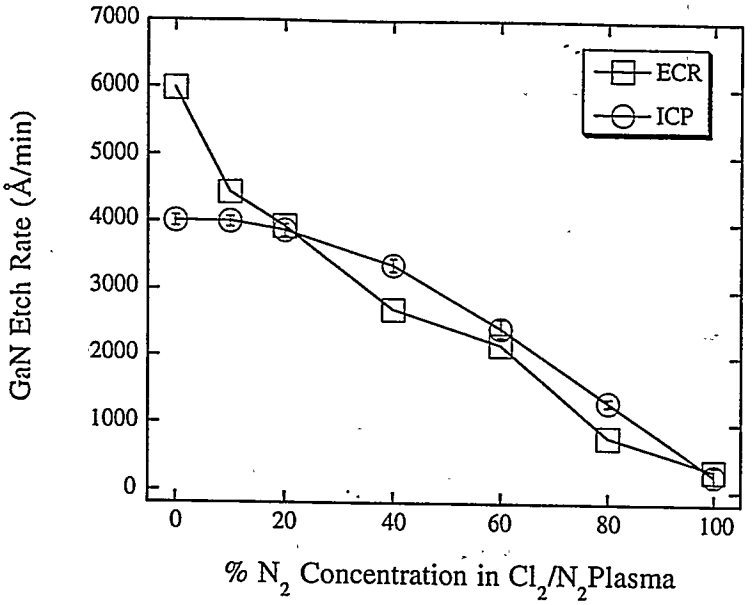

Figure 4. GaN etch rates as a function of $\%N_2$ for ECR- and ICP-generated $Cl_2/N_2/Ar$ plasmas.

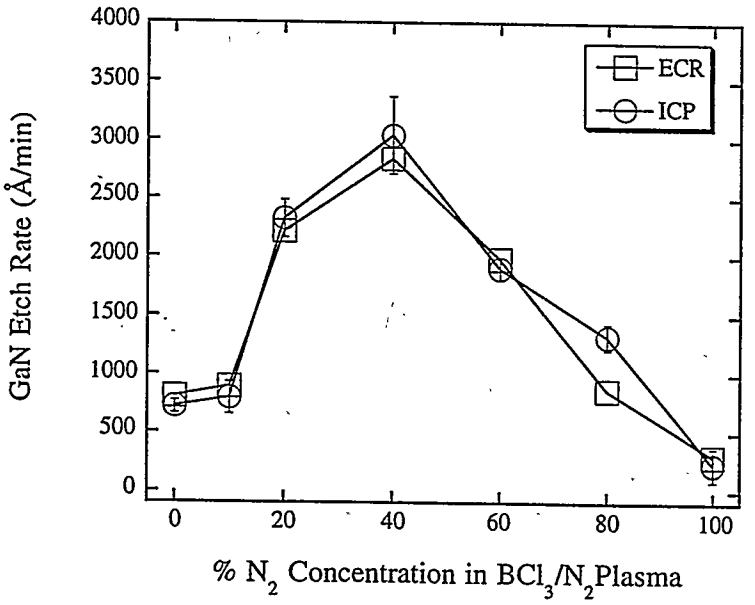

Figure 5. GaN etch rates as a function of %Ar for ECR- and ICP-generated $BCl_3/N_2/Ar$ plasmas.

that observed in ECR and ICP etching of GaAs, GaP, and In-containing materials.[47-49] Ren *et al.* observed peak etch rates for In-containing materials in an ECR plasma at 75% BCl_3- 25% N_2. As N_2 was added to the BCl_3 plasma, Ren observed maximum emission intensity for atomic and molecular Cl at 75% BCl_3 using OES. Correspondingly, the BCl_3 intensity decreased and a BN emission line appeared. It was suggested that at 75% BCl_3, N_2 enhanced the dissociation of BCl_3 resulting in higher concentrations of reactive Cl and Cl ions and higher etch rates. This may explain faster GaN etch rates observed as N_2 was added to the BCl_3/Ar plasmas in this study, however higher concentrations of Cl and BN emission were not observed using OES in the ICP.

In Figure 6, the rms roughness is plotted as a function of $\%N_2$ for the ECR and ICP BCl_3 plasmas. The rms roughness for the as-grown GaN samples etched in the ECR was 1.53 ± 0.06 nm and 3.5 ± 0.2 nm for samples etched in the ICP. The rms roughness for GaN etched in the ECR remained relatively constant (< 2.5 nm) independent of $\%N_2$. The rms-roughness for samples etched in the ICP were slightly higher with the roughest surface (~3.75 nm) at 20% N_2. Figure 7 shows the AFM outputs for GaN etched in ECR-generated BCl_3/N_2 plasmas at 100% BCl_3, 20% N_2/BCl_3, and 60% N_2/BCl_3.

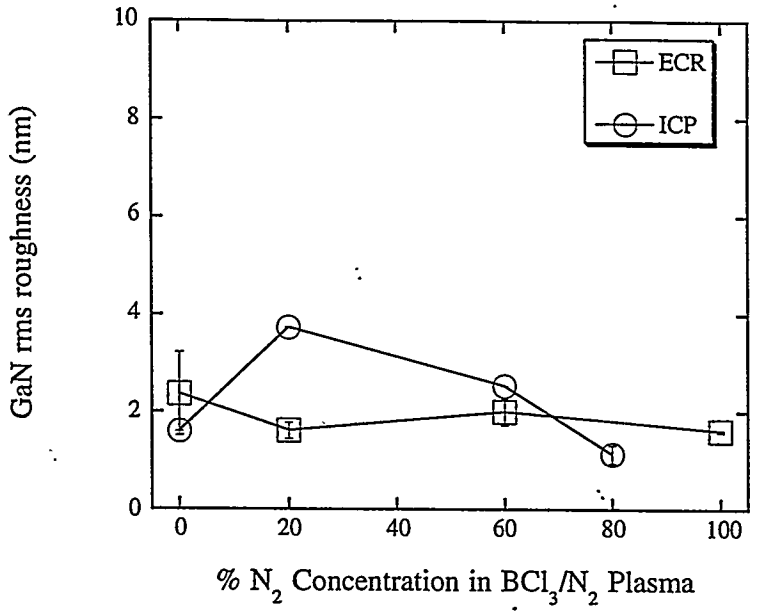

Figure 6. GaN rms-roughness as a function of $\%N_2$ for ECR- and ICP-generated $BCl_3/N_2/Ar$ plasmas.

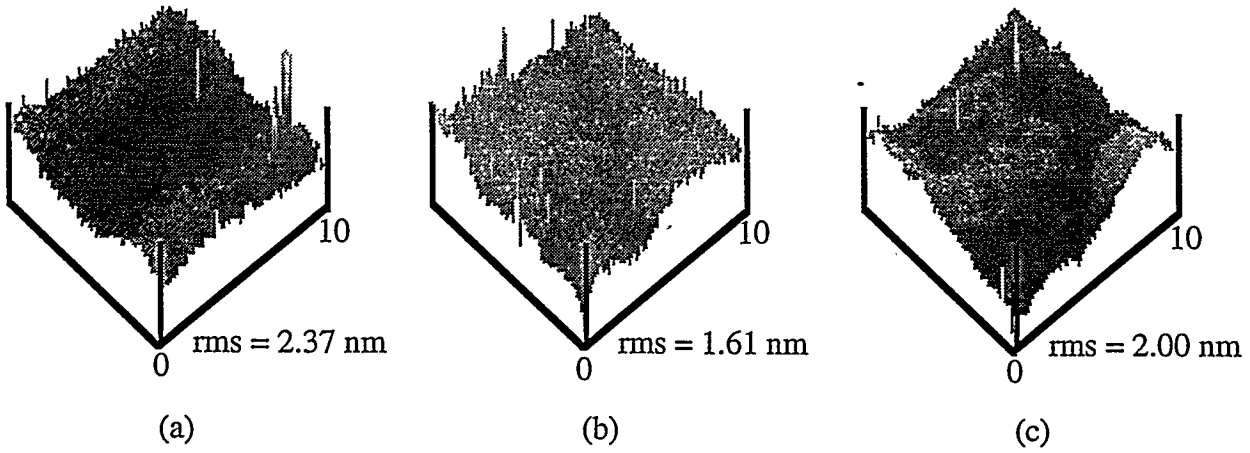

Figure 7. GaN rms-roughness outputs for ECR-generated a) BCl_3 b) 20% N_2/BCl_3, and c) 60% N_2/BCl_3 plasmas. The rms roughness was a) 2.37 ± 0.86 nm, b) 1.61 ± 0.17 nm, and c) 2.00 ± 0.27 nm.

In Figure 8, GaN etch profiles are shown as a function of $\%N_2$ in $BCl_3/N_2/Ar$ ECR- and ICP-generated plasmas. The etched surfaces were relatively smooth independent of $\%N_2$ and etch technique. However, for the ECR-generated 60% N_2/BCl_3 plasma (Figure 8c), significant micromasking was observed possibly due to redeposition. The most anisotropic profiles were

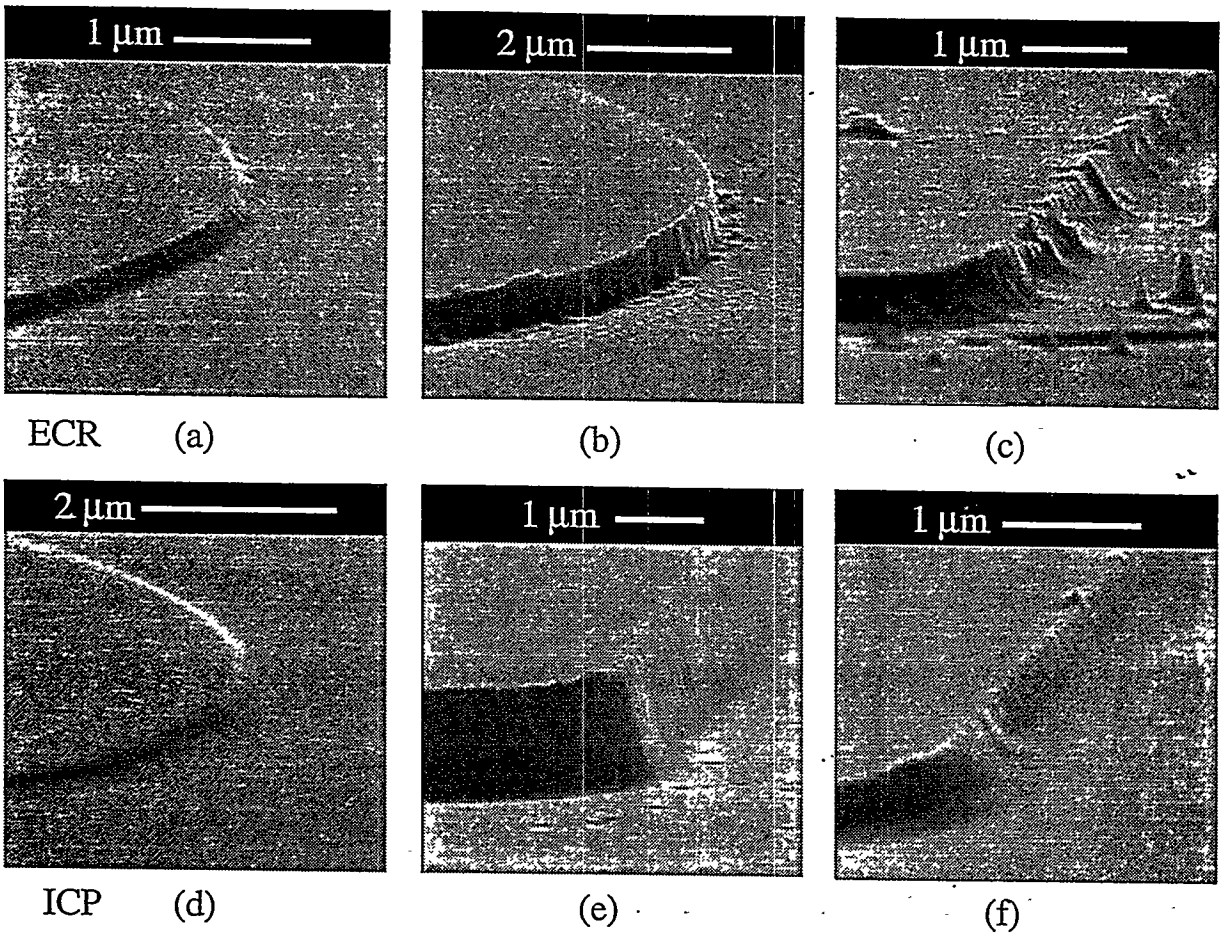

Figure 8. SEM micrographs of GaN samples etched in either an ECR or ICP $BCl_3/N_2/Ar$ plasma at (a, d) 0% N_2 , (b, e) 20% N_2, and (c, f) 60% N_2. The photoresist mask has been removed.

observed at 20% N_2 for both the ECR and ICP (Figures 8b and e). In the pure BCl_3 plasma (Figures 8a and d), the etch depths were quite shallow due to the low concentration of reactive Cl and low GaN etch rate. At 20% N_2, the etch depths and rates were much higher due to higher concentrations of reactive Cl. At high N_2 concentrations (Figures 8c and f), the etch profiles were slightly overcut due possibly to breakdown of the mask-edge.

The addition of H_2 to chlorine-based plasmas typically results in slower etch rates for GaAs and GaP since H_2 acts as a scavenger of reactive Cl and forms HCl. In Figure 9, GaN etch rates are plotted as a function of $\%H_2$ for ECR- and ICP-generated $Cl_2/H_2/Ar$ plasmas. ECR etch conditions were; 1 mTorr pressure, 850 W ECR source power, 150 W rf-cathode-power with corresponding dc-biases of -170 to -210 V, 25 sccm Cl_2/H_2, and 5 sccm Ar. ICP etch conditions were; 2 mTorr pressure, 500 W ICP source power, 95 to 115 W rf-cathode-power with a constant dc-bias of -250 ± 10 V, 25 sccm Cl_2/H_2, and 5 sccm Ar. GaN etch rates in the ECR and ICP increased slightly as H_2 was initially added to the Cl_2/Ar plasma (10% H_2). Using QMS in the ECR discharge, the Cl concentration (m/e = 35) remained relatively constant at 10% H_2. As the H_2 concentration was increased further, the Cl concentration decreased and the HCl concentration increased as the GaN etch rates decreased in both plasmas, presumably due to the consumption of reactive Cl by hydrogen.

In Figure 10, BCl_3 was substituted for Cl_2 and was used to etch GaN in both the ECR and ICP reactors. The increase in etch rate observed at 10% H_2 concentration in the ECR-generated BCl_3 plasma correlated with an increase in the reactive Cl concentration as observed by QMS. As the H_2 concentration was increased further, the Cl concentration decreased, the HCl concentration increased, and the GaN etch rates decreased due to the consumption of reactive Cl by hydrogen. In the ICP reactor, GaN etch rates were quite slow and decreased as H_2 was added to the plasma up to 80% where a slight increase was observed.

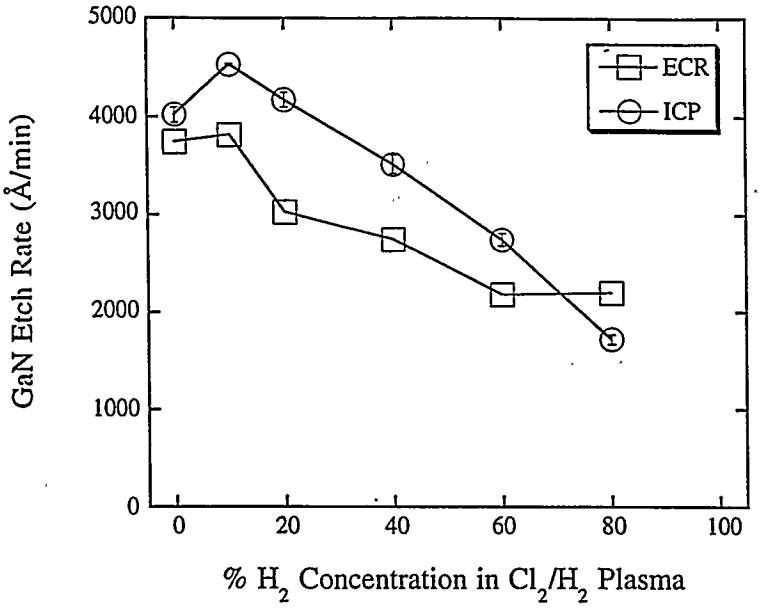

Figure 9. GaN etch rates as a function of $\%H_2$ for ECR- and ICP-generated $Cl_2/H_2/Ar$ plasmas.

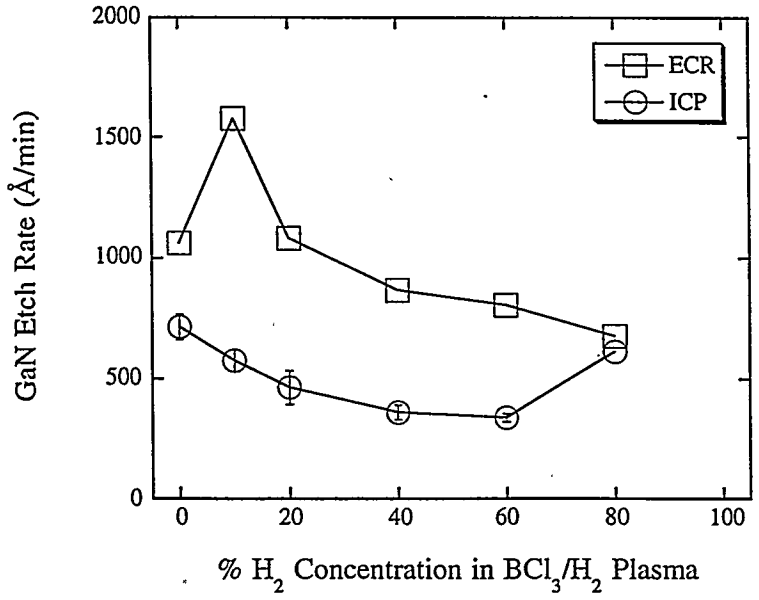

Figure 10. GaN etch rates as a function of $\%H_2$ for ECR- and ICP-generated $BCl_3/H_2/Ar$ plasmas.

Auger spectra for GaN samples etched under several different ICP plasma conditions were taken to determine the near-surface stoichiometry. The Auger spectrum for the as-grown GaN showed normal amounts of adventitious carbon and native oxide on the GaN surface. Following exposure to either a Cl_2- or BCl_3-based plasma, Cl and/or B were observed on the surface. The Ga:N ratios for samples exposed to a plasma were normalized to the ratio of the as-grown sample. For GaN samples etched in $Cl_2/H_2/Ar$ or $Cl_2/N_2/Ar$ plasmas, the normalized Ga:N ratio remained relatively constant ranging from ~0.9 to 1.25. The ratios approached 1 at 60% H_2 or N_2 implying equi-rate removal of Ga and N. For the BCl_3-based plasmas, the normalized Ga:N ratios decreased at 20% H_2 and N_2 and then increased at 60%. At 20% N_2/BCl_3, the surface was N-rich,

whereas all other surfaces were Ga-rich. GaN surfaces exposed to BCl_3-based plasmas showed consistently higher ratios as compared to Cl_2-based plasmas due to the more physical nature of the etch mechanisms.

Figure 11 shows a SEM micrograph of GaN etched in a $Cl_2/H_2/Ar$ ICP-generated plasma. The plasma conditions were; 5 mTorr pressure, 500 W ICP power, 22.5 sccm Cl_2, 2.5 sccm H_2, 5 sccm Ar, 25°C temperature, and a dc-bias of -280 ± 10V. Under these conditions the GaN etch rate was ~6880 Å/min with highly anisotropic, smooth sidewalls. The vertical striations observed in the sidewall were due to striations in the photoresist mask which were transferred into the GaN feature during the etch. The sapphire substrate was exposed during the overetch period and showed significant pitting possibly due to defects in the substrate or growth process.

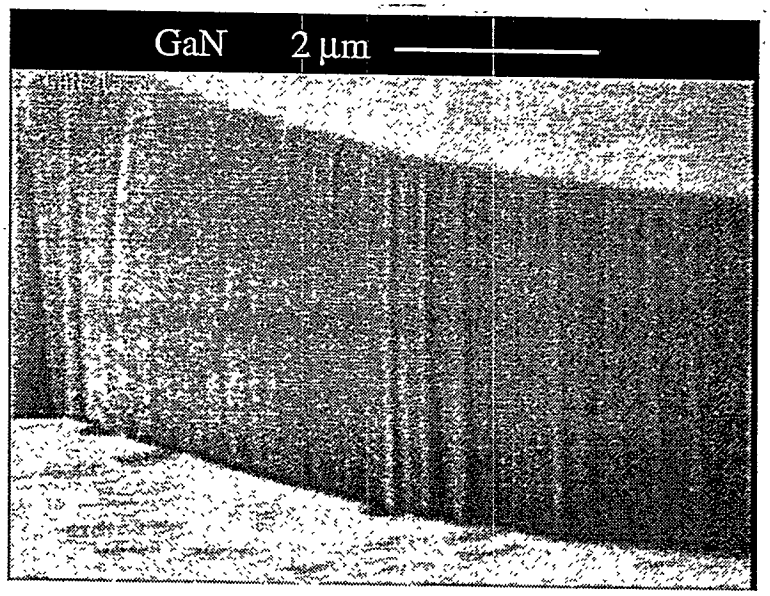

Figure 11. SEM micrograph of MOCVD GaN etched in an ICP-generated $Cl_2/H_2/Ar$ plasma.

CONCLUSIONS

In summary, the utilization of high-density ECR and ICP chlorine-based plasmas has resulted in high rate (> 0.5 μm/min), smooth, anisotropic etching of GaN. The source of reactive Cl (Cl_2, BCl_3, ICl, etc.) and the use of additive gases (Ar, H_2, N_2, SF_6, etc.) have several effects on the etch characteristics of GaN. Cl_2-based plasmas typically resulted in faster GaN etch rates as compared to BCl_3-based plasmas due to higher concentrations of reactive Cl. The addition of SF_6, N_2, or H_2 to Cl_2- or BCl_3-based plasmas appeared to effect the concentration of reactive Cl in the plasma which directly correlated to the GaN etch rate. GaN etch rate trends were quite similar for ICP and ECR reactors independent of plasma chemistry. Very smooth pattern transfer was obtained over a wide range of plasma chemistries. The mechanism of breaking the GaN bonds appears to be critical and perhaps the rate limiting step in the etch mechanism. The use of high-density plasmas resulted in improved GaN etch results possibly due to a two step process directly related to the plasma flux. Initially the high-density plasmas increase the bond breaking mechanism allowing the etch products to form and then produce efficient sputter desorption of the etch products. ICP etching of the group-III nitrides in Cl_2/H_2 plasmas resulted in etch profiles and sidewall smoothness which may improve the yield and performance of etched facet lasers.

ACKNOWLEDGMENTS

The authors would like to thank P. L. Glarborg and L. Griego for their technical support. This work was performed at Sandia National Laboratories supported by the U.S. Department of Energy under contract # DE-AC04-94AL85000. Sandia is a multiprogram laboratory operated by Sandia Corporation, a Lockheed Martin Company, for the United States Department of Energy.

REFERENCES

1. S. Nakamura, T. Mukai, and M. Senoh, Jpn. J. Appl. Phys. **30**, L1998 (1991).
2. S. Nakamura, T. Mukai, M. Senoh, and N. Iwasa, Jpn. J. Appl. Phys. **31**, L139 (1992).
3. J. S. Foresi and T. D. Moustakas, Appl. Phys. Lett. **62**, 2859 (1993).
4. S. C. Binari, L. B. Rowland, W. Kruppa, G. Kelner, K. Doverspike, and D. K. Gaskill, Electron. Lett. **30**, 1248 (1994).
5. S. Nakamura, T. Mukai, and M. Senoh, Appl. Phys. Lett. **64**, 1687 (1994).
6. S. Nakamura, M. Senoh, N. Iwasa, and S. Nagahama, Jpn. J. Appl. Phys. **34**, L797 (1995).
7. S. Nakamura, M. Senoh, S. Nagahama, N. Iwasa, T. Yamada, T. Matsushito, H. Kiyoku, and U. Sugimoto, Jap. J. Appl. Phys. **35**, L74 (1996).
8. T. Matsuoka, T. Sasaki, and A. Katsui, Optoelectronic Devices and Technologies **5**, 53 (1990).
9. H. Amano, M. Kito, K. Hiramatsu, and I. Akasuki, Jpn. J. Appl. Phys. **28**, L2112 (1989).
10. S. Strite and H. Morkoc, J. Vac. Sci. Technol. B **10**, 1237 (1992).
11. M. A. Kahn, J. N. Kuzina, J. M. Van Hove, D. T. Olson, S. Krishnankutty, and R. M. Kolbas, Appl. Phys. Lett. **58**, 526 (1991).
12. M. A. Khan, A. Bhattarai, J. N. Kuznia, and D. T. Olson, Appl. Phys. Lett. **63**, 1214 (1993).
13. R. F. Davis. Proc. IEEE **79**, 702 (1991).
14. I. Akasaki, H. Amano, M. Kito, and K. Kiramatsu, Lumin. **48/49**, 666 (1991).
15. M. A. Khan, Q. Chen, M. S. Shur, B. T. Dermott, J. A. Higgins, J. Burm, W. Schaff, and L. F. Eastman, Electron. Lett. **32**, 257 (1996).
16. J. C. Zolper, R. J Shul, A. G. Baca, R. G. Wilson, S. J. Pearton, and R. A. Stall, Appl. Phys. Lett. **68**, 2273 (1996).
17. see for example, *High-density Plasma Sources,* ed. O. A. Popov (Noyes Publications, Park Ridge, NJ, 1996).
18. M. A. Lieberonan and R. A. Gottscho, in *Plasma Sources for Thin Film Deposition and Etching*, ed. M. H. Francombe and J. L. Vossen, Physics of Thin Films Vol. 18 (Academic Press, San Diego, 1994).
19. T. L. Chu, J. Electrochem. Soc. **119**, 1200 (1971).
20. J. I. Pankove, J. Electrochem, Soc. **119**, 1118 (1972).
21. Q. X. Guo, O. Kato, and A. Yoshida, J. Electrochem. Soc. **139**, 2008 (1992).
22. S. J. Pearton, C. R. Abernathy, F. Ren, J. R. Lothian, P. W. Wisk, and A. Katz, J. Vac. Sci. Technol. **A11**, 1772 (1993).
23. T Y. Sheng, Z. Q. Yu, and G. J. Collins, Appl. Phys. Lett. **52**, 576 (1988).
24. T. Pauleau, J. Electrochem. Soc. **129**, 1045 (1982).
25. K. M. Taylor, and C. Lenie, J. Electrochem. Soc. **107**, 308 (1960).
26. G. Long and L. M. Fuster, J. Am. Ceram. Soc. **42**, 53 (1959).
27. N. J. Barrett, J. D. Grange, B. J. Sealy, and K. G. Stephens, J. Appl. Phys. **57**, 5470 (1985).
28. C. R. Aita and C. J. Gawlak, J. Vac. Sci. Technol. **A1**, 403 (1983).
29. G. R. Kline and K. M. Lakin, Appl. Phys. Lett. **43**, 750 (1983).
30. J. R. Mileham, S. J. Pearton, C. R. Abernathy, J. D. MacKenzie, R. J. Shul, and S. P. Kilcoyne, J. Vac. Sci. Technol. **A14**, 836 (1996).
31. I. Adesida, A. Mahajan, E. Andideh, M. Asif Khan, D. T. Olsen, and J. N. Kuznia, Appl. Phys. Lett. **63**, 2777.
32. M. E. Lin, Z. F. Zan, Z. Ma. L. H. Allen, and H. Morkoc, Appl. Phys. Lett. **64**, 887 (1994).
33. A. T. Ping, I. Adesida, M. Asif Khan, and J. N. Kuznia, Electron. Lett. **30**, 1895 (1994).
34. H. Lee, D. B. Oberman, and J. S. Harris, Jr., J. Electron. Mat. **25**, 835 (1996).
35. C. B. Vartuli, S. J. Pearton, J. W. Lee, J. Hong, J. D. MacKenzie, C. R. Abernathy, and R. J. Shul, Appl. Phys. Lett. **69**, 1426 (1996).
36. C. B. Vartuli, J. D. MacKenzie, J. W. Lee, C. R. Abernathy, S. J. Pearton, and R. J. Shul, J. Appl. Phys. **80**, 3705 (1996).
37. S. J. Pearton, C. R. Abernathy, and F. Ren, Appl. Phys. Lett. **64**, 2294 (1994).

38. S. J. Pearton, C. R. Abernathy, and F. Ren, Appl. Phys. Lett. **64**, 3643 (1994).
39. R. J. Shul, S. P Kilcoyne, M. Hagerott Crawford, J. E. Parmeter, C. B. Vartuli, C. R. Abernathy, and S. J. Pearton, Appl. Phys. Lett. **66**, 1761 (1995).
40. L. Zhang, J. Ramer, J. Brown, K. Zheng, L. F. Lester, and S. D. Hersee, Appl. Phys. Lett. **68**, 367 (1996).
41. R. J. Shul, A. J. Howard, S. J. Pearton, C. R. Abernathy, C. B. Vartuli, P. A. Barnes, and M. J. Bozack, J. Vac. Sci. Technol. **B13**, 2016 (1995).
42. G. F. McLane, L. Casas, S. J. Pearton, and C. R. Abernathy, Appl. Phys. Lett. **66**, 3328 (1995).
43. I. Adesida, A. T. Ping, C. Youtsey, T. Dow, M. Asif Khan, D. T. Olson, and J. N. Kuzina, Appl. Phys. Lett **65**, 889 (1994).
44. R. J. Shul, G. B. McClellan, S. A. Casalnuovo, D. J. Rieger, S. J. Pearton, C. Constantine, C. Barratt, R. F. Karlicek, Jr., C. Tran, and M. Schurman, Appl. Phys. Lett. **69**, 1119 (1996).
45. H. P. Gillis, D. A. Choutov, and K. P. Marlin, JOM, 50 (1996).
46. S. J. Pearton and R. J. Shul, "III-Nitrides", Academic Press, in press.
47. F. Ren, J. R. Lothian, J. M. Kuo, W. S. Hobson, J. Lopata, J. A. Caballero, S. J. Pearton, and M. W. Cole, J. Vac. Sci. Technol. **B14**, 1 (1995).
48. F. Ren, W. S. Hobson, J. R. Lothian, J. Lopata, J. A. Caballero, S. J. Pearton, and M. W. Cole, Appl. Phys. Lett. **67**, 2497 (1995).
49. R. J. Shul, G. B. McClellan, R. D. Briggs, D. J. Rieger, S. J. Pearton, C. R. Abernathy, J. W. Lee, C. Constantine, and C. Barratt, J. Vac. Sci. and Technol. A, in press, (1996).